A Critical Look at Some Conceptual Aspects of Kinetic Theories of Polymer Crystal Growth

J. J. Point

Service de Chimie Physique et de Thermodynamique, Université de l'Etat à Mons, Belgique

A. J. Kovacs*

CNRS-ULP, Centre de Recherches sur les Macromolécules, 67083 Strasbourg, France.
Received July 11, 1979

ABSTRACT: Application of current kinetic theories of polymer crystal growth, based on coherent surface nucleation and subsequent sequential deposition of chain segments, is extended to short chain molecules, while accounting for the effect of chain ends in a consistent manner. The relevant expressions for the growth rate are compared with the experimental data obtained with a series of low molecular weight (2000–10 000) poly(ethylene oxide) fractions reported previously. This comparison is achieved by using a set of reduced variables which eliminate some of the unknown parameters appearing in the theoretical expressions, and it reveals some important and irreducible discrepancies between theory and experiment. The latter clearly originate from the failure of the basic postulates of the theoretical model to describe the actual mechanism of polymer crystal growth.

Kinetic theories of polymer crystal growth have been proposed by several authors[1-3] in the early 60's to account for Keller's discovery[4] that solution grown polyethylene single crystals are made of chains in a folded conformation. These theories, based on coherent surface nucleation, imply sharp molecular folds with adjacent re-entry and yield expressions for the temperature dependence of the lamellar thickness, l, and the growth rate, G, of the crystals, both depending on the actual undercooling of the system.

Since their early formulation, these treatments have been supposed to account for a great variety of fragmentary experimental results obtained with linear polymers in a wide temperature range, whether the crystals grow from dilute solution[1] or from the melt.[2] Accumulation of the experimental data made it necessary, however, to introduce further sophistication and additional parameters in the original theory in order to maintain its applicability without restriction. A comprehensive review of the present status of these treatments has been given recently by Hoffman, Davis, and Lauritzen,[5] and their statements will be repeatedly referred to in the analysis given below.

During recent years, however, increasing evidence has been accumulated by means of small-angle neutron scattering, showing that the chain conformations in solution and melt-crystallized polymers are not alike[6] and that melt crystallization does not alter significantly the radius of gyration of the chains from that in the liquid state, where they have a random coil conformation. These findings are, of course, in formal contradiction with the unifying concept of adjacent chain re-entry implied by the theory, although reasonable agreement has been claimed between the values of the theoretical parameters determining l and G in both solution and melt-crystallized specimens.[5]

This paradoxical situation led us to submit the basic concepts of the theory to a critical examination, using a rather exhaustive set of data[7-10] on the growth rate and lamellar thickness of melt grown single crystals of low molecular weight poly(ethylene oxide) (PEO) fractions. In this context we will first extend the application of the theory to short chains and derive an expression for the growth rate of fully extended chain crystals, which do not raise problems about chain folding. This expression for G results in a simple reduction rule, from which one can easily determine the lateral surface energy (σ) involved in the crystallographic attachment of a new chain segment onto the growth face. The value of this important parameter is then evaluated by comparing the extended chain crystal growth rates displayed by any two PEO fractions at corresponding undercoolings defined by the reduction rule. The comparison reveals unambiguously some fundamental inconsistency in the coherent surface nucleation concept, and the discrepancy cannot be removed by any sound modification of the present theoretical approaches. This conclusion is further substantiated by the analysis of the growth rate of folded chain PEO crystals. Finally, it will be shown that for a given fraction, the actual thermal variation of G cannot be reconciled with the theoretical predictions.

Materials and Data Used in the Analysis

The data considered here concern the growth and melting behavior of melt-growth single crystals of narrow, hydroxy-terminated PEO fractions, ranging between 2000 and 10 000 in the number average molecular weight (M_n), listed in Table I. These fractions crystallize from the undercooled melt with chains either fully extended or folded a small number, n, of times.[11] In addition, the chain ends are rejected onto the surface layers of the crystalline lamellae and the helical chain axis is normal to the latter.[8] Therefore, the lamellar thickness

$$l(n,p) = L(1 + n)^{-1} \equiv pl_u(1 + n)^{-1} \quad (1)$$

is an *integral submultiple* of the overall chain length, L (in the crystal lattice), which is proportional to the number average degree of polymerization p (see Table I), the proportionality factor being $l_u = 0.2783$ nm, i.e., the length of one monomer unit along the chain axis, parallel to the c axis of the PEO subcell.[12]

The number (n) of folds per molecule depends on crystallization temperature and time. In fact, during isothermal crystallization (or annealing) the lamellar thickness increases in a stepwise manner, due to the quantized reduction of n. The lamellar thickness of such crystals can thus be determined unambiguously by means of three independent methods: (i) small-angle X-ray scattering (often displaying reflections up to the fifth order[11]), (ii) electron microscopy of surface replicas or shadowed individual crystals grown from thin molten layers, and (iii) molecular weight determination (provided that n is known). In most cases, the agreement between the l values obtained by these methods is better than about 5%, though fractionation occurring during slow crystallization

0024-9297/80/2213-0399$01.00/0

Table I
Characteristic Parameters of the PEO Fractions[8,9]

POE	M_n	M_w/M_n[a]	p	L,[b] nm	$T^*(0,p)$, °C	$T_m(n,p)$, °C[c]			$p[T_m(\infty) - T_m(n,p)]/T_m(n,p)$		
						$n = 0$	$n = 1$	$n = 2$	$n = 0$	$n = 1$	$n = 2$
a (2000)	1890	1.27	43	12.0	42.0	52.7			2.14		
b (3000)	2780	1.08	63	17.5	50.0	57.6			2.15		
c (4000)	3900	1.11	89	24.8	54.9	60.4	55.9		2.27	3.52	
d (6000)	5970	1.06	136	37.8	59.4	63.3	60.7	59.0	2.26	3.34	4.05
e (8000)	7760	1.19	176	49.0	61.8	64.3	62.5	61.0	2.40	3.36	4.16
f (10000)	9970	1.20	227	63.2	63.2	65.4	64.0	62.9	2.35	3.30	4.05

[a] M_w/M_n: the weight and number average molecular weight ratio. [b] Calculated from eq 1; $L = pl_u$. [c] DSC data.[14]

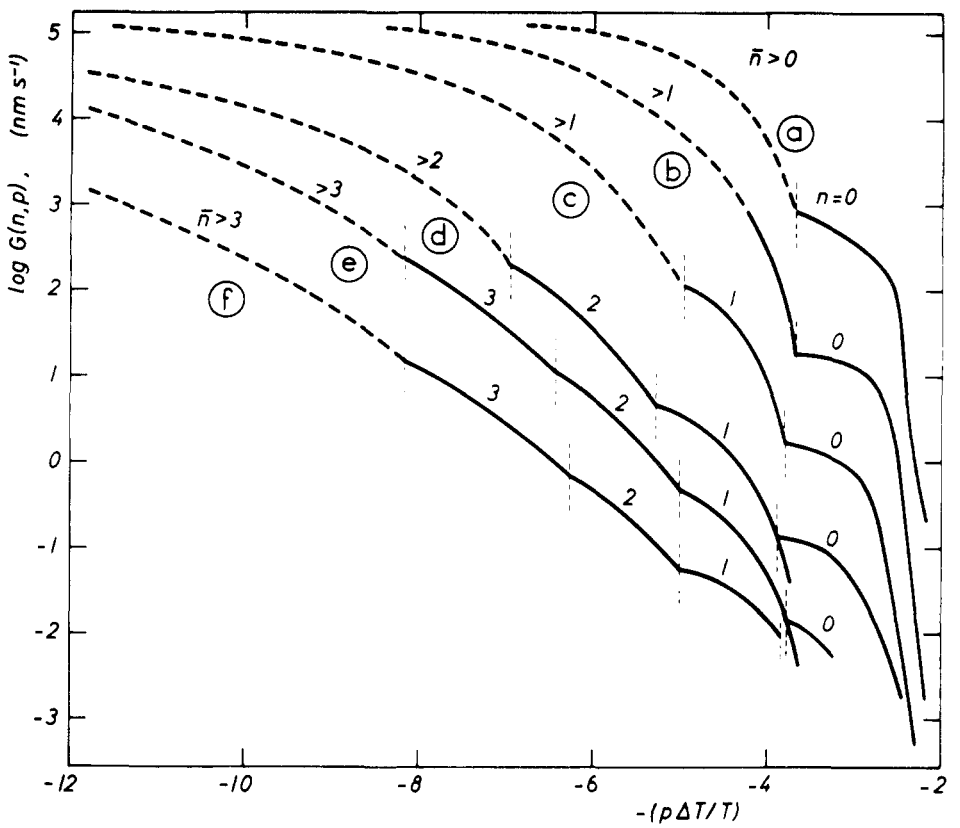

Figure 1. Dependence of the crystal growth rate $G(n,p)$ of various PEO fractions (see Table I) on the reduced undercooling, $p\Delta T/T$, with $\Delta T = T_m(\infty) - T$. Growth transition temperatures $T^*(n,p)$ are indicated by vertical dashed lines. The growth branches obtained at relatively large undercoolings, shown by dashed lines, are relevant to the growth of highly unstable ("ephemeral") crystals[9] in which the chain conformation readily transforms into the next nearest metastable form, involving the largest integral number (n) of folds determined by the chain length.[14]

may introduce a larger discrepancy.[11]

Concomitantly, the crystal melting temperature $T_m(n,p)$ also depends on the two independent molecular parameters p and n, characterizing the average length of the chains and their overall conformation in the crystal, respectively. The melting temperatures $T_m(n,p)$ as determined by differential scanning calorimetry[13,14] and in some cases (n = 0 and 1) from the zero growth criterion[8,9] (see below) are listed in Table I. They have also been interpreted[13,14] theoretically by using an approach similar to that of Flory and Vrij,[15] thus including in the free energy balance the entropy of localization of the chain ends after crystallization. This term amounts to kT ln Cp per chain, C^{-1} being the number of monomer units in the statistical segment, characterizing the chain flexibility. This term will also be introduced in the free energy balance of the growth nucleus given below, since it appeared to be essential in accounting accurately for the observed variations of $T_m(n,p)$. The analysis of these variations leads further to an estimation of the surface free energies of the chains ends $\sigma_{e,e}$ and chain folds $\sigma_{e,f}$, both located in the surface layers of the lamellae. The values of $\sigma_{e,e}$ and $\sigma_{e,f}$ together with other thermodynamic parameters[13,14] relevant to the present analysis are listed in Appendix I.

Growth, thickening, and melting behavior of PEO single crystals have been investigated in a systematic manner.[7-9] Figure 1 shows the growth rate (G) data obtained with six fractions plotted as a function of $p\Delta T/T$, where $\Delta T = T_m(\infty) - T$ is the undercooling with respect to $T_m(\infty)$ = (68.9 ± 0.4) °C, the equilibrium melting temperature of a large and perfect extended chain crystal composed of very long chains,[13] and T is the crystallization temperature. These data refer to the growth of the (010) prism face; data relevant to the (100) or {140} prism faces differ only slightly from those shown in Figure 1.

Clearly, each curve in Figure 1 consists of juxtaposed "hyperbolic" branches which intersect at precisely defined growth transition temperatures[7-9] $T^*(n,p)$ (relevant to the (010) face and shown by vertical dashed lines), below which growth proceeds with (n + 1) times folded chains, while the negative temperature coefficient $-\mathrm{d} \log G/\mathrm{d}T = \mathrm{d} \log G/\mathrm{d}(\Delta T)$ displays a stepwise and often considerable in-

crease. In addition, in a narrow temperature interval (~0.1 K) near $T^*(0,p)$, the morphology and crystal habit display some spectacular modifications ("pathological" crystals[8]) which accompany the transition from once folded to extended chain crystal growth for each $hk0$ prism face.[10]

Accordingly, each $G(n,p)$ branch can be characterized by the number of folds involved in the growth process, as indicated in Figure 1. For $n = 0$, these branches closely approach the melting temperature $T_m(0,p)$ and for two fractions (d and e) even the branches obtained for $n = 1$ could be extended above $T^*(0,p)$ near to $T_m(1,p)$. In the narrow temperature interval $T^*(0,p) \rightarrow T_m(1,p)$, one can thus grow either extended or once folded chain crystals, depending on the thickness of the seed crystals on which the chains deposit. In fact, it has been shown that extended chain crystals cannot grow upon a once folded chain substrate.[8,9]

Clearly, the data shown in Figure 1 provide a challenging and, at present, unique experimental framework for theoretical speculations. In addition, the variation of the growth rate (of known prism faces) covers a wide range (about six decades), and for each $G(n,p)$ branch the fold length generated by growth is precisely defined, while its changes at $T^*(n,p)$ are discontinuous and large. Furthermore, the number of folds is small ($n < 4$) and chain folding, if any, presumably involves adjacent re-entry. The temperature interval of interest is small so that the thermal variation of the relevant thermodynamic parameters can be ignored. Finally, the chains are relatively short and chain entanglements are absent in the melt.[25] Other, more specific properties of these systems will be further recalled when relevant to the analysis which follows.

Theoretical

In this section the formulation of the classical theory will first be adapted to the formation of a growth nucleus made of short chains, while accounting for the effect of chain ends in a consistent manner, as suggested by one of us in a previous paper (see the Appendix in ref 9). The theory is applied to the growth of extended chain PEO crystals yielding a simple reduction rule which enables one to compare the growth rates of the different fractions at corresponding undercoolings. This results in the evaulation of the lateral surface free energy, independently of the values of the other parameters, which cannot be determined directly from experiment. The evaluation of σ reveals some physical inconsistency in the basic concept of the theoretical model. The discrepancy between theory and experiment is further substantiated by the analysis of the growth rate of folded chain PEO crystals.

Adaptation of the Theory to Crystallization of Short Chains. In the classical treatments of polymer crystal growth, based on coherent surface nucleation,[1-3,17] the formation of the surface nucleus is assumed to be a sequential process. The first and most critical step controlling the rate of crystal growth is the crystallographic attachment of the first stem of length l onto the relevant prism face (Figure 2a), assumed to be even and smooth. In this step the variation of the free energy $\Delta\phi_0$ of the chain (with reference to the melt) can be written as

$$\Delta\phi_0 = 2bl\sigma - \psi\Delta F_c(l,T) + \alpha 2ab\sigma_e > 0 \qquad (2)$$

where a, b, and l represent the geometrical dimensions of the stem and σ and σ_e are the relevant surface free energies per unit area.

The first term of $\Delta\phi_0$ is positive and corresponds to the creation of the new surfaces $2bl$ (Figure 2a), σ being the free energy per unit area of the *lateral* surface, assumed again to be regular and smooth.

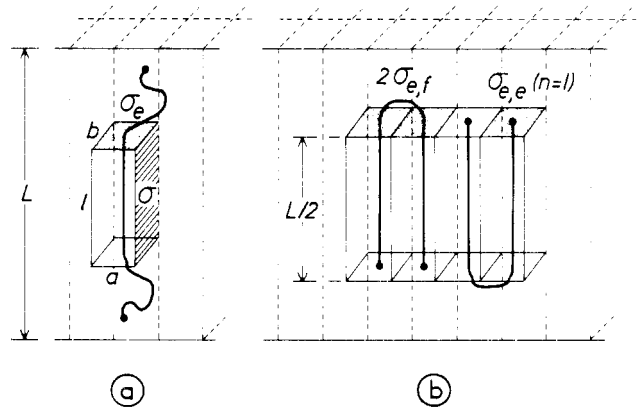

Figure 2. (a) Crystallographic deposition of a single stem onto the growth face. (b) Chain conformation in once folded chain nuclei ($n = 1$) and the relevant surface free energies.

The second term, $\psi\Delta F_c(l,T)$, represents (at T) the bulk free energy of crystallization relevant to the stem of length $l \leq L$. The apportionating factor ψ, ranging from zero to unity, has been introduced by Lauritzen and Hoffman[17] and interpreted in terms of physical adsorption of the chain segments prior to their crystallographic attachment onto the growth face (see Figures 26 and 27 in ref 5). Accordingly, $\psi = 1$ implies no absorption and $\psi = 0$ implies total adsorption prior to crystallographic attachment. As alluded to above, it will be further assumed in the case of short chains that the term $\Delta F_c(l,T)$ also includes the entropy of localization of the chain[15] which is negative and amounts to $-k \ln Cp$ per molecule. Apportionating this entropy to the fractional length (l/L) of the chain,[26] one can write, omitting the (l,T) functionality

$$\Delta F_c \equiv \Delta F_c(l,T) = abl\Delta f - kT(l/L) \ln Cp \qquad (3)$$

where Δf is the bulk free energy of crystallization per unit volume. For moderate undercoolings, this can be approximated by

$$\Delta f \simeq \Delta h_f[T_m(\infty) - T]/T_m(\infty) \equiv \Delta h_f \Delta T/T_m(\infty) \qquad (4)$$

in which Δh_f is the enthalpy of fusion per unit volume of a perfect crystal and $T_m(\infty)$ is the equilibrium melting temperature of a large crystal containing neither chain ends nor chain folds, since all the surface effects are accounted for by the first and third terms of eq 2.

In the third term $2ab\sigma_e$ represents the excess free energy associated with the two dangling chain ends (or cilia) exceeding the length l of the stem (cf. Figure 2a) and involving a surface free energy σ_e which depends on the lengths of the nonattached chain segments. This term has been considered in the early treatments,[1-3] but it has been omitted, without justification, in the more recent versions of the theory given by Lauritzen and Hoffman.[5,17] In the present context we consider this term to be essential. Nevertheless, in the expressions of the rate of chain deposition given below (cf. eq 5 and 7) we will bias it by a factor α similar to ψ ($0 < \alpha \leq 1$), in order to account for a possible asymmetry of the activation barrier associated with $2ab\sigma_e$.

The free energy change $\Delta\phi_0$ relevant to the crystallization of the first stem thus takes into account all the effects which can be associated with the model (Figure 2a). Expressions similar to eq 2 have also been considered by others,[18,19] leading basically to the same results, as has been shown recently by Labaig.[20] Nevertheless, in the treatment proposed by Hoffman et al.[21] for the growth of polyethylene crystals made of short chains, the entropy of localization (cf. eq 3) and the effects of chain ends ($2ab\sigma_e$)

are both neglected in the expression of $\Delta\phi_0$. This omission, however, has been partly compensated for in defining the undercooling by $\Delta T' = T_m(0,p) - T$, which appears inconsistent with the theoretical model[9,20] and leads to an underestimation of the value of σ_e.

It should be pointed out that $\Delta\phi_0$ must be positive in order to prevent the nucleation frequency, and thus the growth rate, from increasing with l. In fact, the reduction factor ψ of ΔF_c has been introduced by Lauritzen and Hoffman[17] in order to maintain $\Delta\phi_0$ positive even for large undercoolings, thus to shift the "δl catastrophe" to sufficiently low temperatures[5,17] (see below).

Accordingly, the rate of deposition A_0 of the first stem can be expressed as

$$A_0 = \beta \exp(-\Delta\phi_0/kT) = \beta \exp[(-2bl\sigma + \psi\Delta F_c - \alpha 2ab\sigma_e)/kT] \quad (5)$$

where β includes the usual frequency factor (kT/h) and the energy barriers associated with the chain transport from the liquid to the solid substrate. These factors have been discussed in detail by Hoffman et al.[5] and owing to their relative insensitivity to small temperature changes they will not be further considered, except for their possible molecular weight dependence, to be discussed below.

On the other hand, the rate constant B_1, corresponding to the full detachment of the first stem, involves terms similar to A_0, but of opposite sign, and can be written as

$$B_1 = A_0 \exp[(2bl\sigma - \Delta F_c + 2ab\sigma_e)/kT] = \beta \exp\{[-(1-\psi)\Delta F_c + (1-\alpha)2ab\sigma_e]/kT\} \quad (6)$$

The formation of the growth nucleus proceeds by attachment of additional stems of length l in an *adjacent position* to the first (otherwise the rate constants would be identical with those involved in the first stem and result in a further increase of $\Delta\phi$, thus preventing growth). Then the relevant forward and backward reaction rates can be expressed by

$$A = \beta \exp[(\psi\Delta F_c - \alpha' 2ab\bar{\sigma}_e)/kT] \quad (7)$$

$$B = \beta \exp\{[-(1-\psi)\Delta F_c + (1-\alpha')2ab\bar{\sigma}_e]/kT\} \quad (8)$$

where $2ab\bar{\sigma}_e$ represents the average value of the basal surface free energy per stem. In fact, $\bar{\sigma}_e$ generally takes values different from that involved in the attachment of the first stem, since for short chains the additional stems may include either chain ends or folds or other types of crystal defects. The reduction factor α' associated with $\bar{\sigma}_e$ is generally assumed to be equal to unity.[3,5,17]

The necessary requirement for the growth nucleus to develop is clearly given by $(A/B) > 1$, viz.,

$$\Delta F_c \equiv \Delta F_c(l,T) > 2ab\bar{\sigma}_e \quad (9)$$

Note that this inequality is independent of σ and of the values of the apportionating factors ψ and α'. Since attachment of the successive stems proceeds by periodic deposition of individual chains, one can average the free energies involved by multiplying both members of the inequality by L/l to obtain (cf. eq 3)

$$(L/l)\Delta F_c = abL\Delta f - kT \ln Cp > 2abL\bar{\sigma}_e/l \equiv ab\sum_e(\bar{n}) \quad (10)$$

in which the last member represents the surface free energy relevant to one $\bar{n}$-times folded chain in the growth nucleus, $\bar{n}$ being the average number of folds per molecule in a nucleus of length $L(1+\bar{n})^{-1}$.

Of course, when $A < B$, melting rather than growth occurs and the limiting condition $A = B$ corresponds to the equilibrium situation defining the zero growth criterion,[8,14] for which one has (cf. eq 4)

$$abL\Delta h_f[T_m(\infty) - T_m(\bar{n},p)]/T_m(\infty) - kT_m(\bar{n},p) \ln Cp = ab\sum_e(\bar{n}) \quad (11)$$

where $T_m(\bar{n},p)$ is the melting temperature of the particular crystal involving $\bar{n}$ folds per chain. Equations 10 and 11 thus define the requirement for growth and the concomitant melting temperature of these crystals in a self-consistent manner.

Flux and Growth Regime. The next step in the problem is to express the flux $S(l)$ over the nucleation barrier to generate a monomolecular layer of thickness b and of length l (Figure 2). In steady state conditions this flux is determined by the various forward and backward reaction rates considered above, yielding[5,17]

$$S(l) = N_0A_0(A - B)/(A - B + B_1) \quad (12)$$

where N_0 is the occupation number for the first stem. The total flux, S_T, controlling the growth rate is then given by summing over all possible values of l, ranging from a minimum (determined by eq 9; $\Delta F_c(l_{min},T) = 2ab\bar{\sigma}_e$) to L, viz.,

$$S_T = \sum_{l_{min}}^{L} S(l) \equiv l_u^{-1} \int_{l_{min}}^{L} S(l)\, dl \quad (13)$$

where the sum is replaced by an integral. This is equivalent to assuming that the possible values of l are integer multiples of the length l_u of one repeat unit and that $S(l)$ can be considered as a smooth function of l.

Furthermore, one can envisage two growth regimes depending on whether the attachment of the first stem is sufficient to induce rapid deposition of the others to form a monomolecular layer in the prism face considered (mononucleation or regime I) or else nucleation starts quasi-simultaneously from many equivalent sites of the growth face (multinucleation or regime II). In both cases G is simply related to the total flux S_T, since one can derive by strict argument[17,18] for regimes I and II

$$G_I \propto S_T \text{ and } G_{II} \propto [S_T(A - B)]^{1/2} \quad (14)$$

in which the proportionality factors have been omitted for simplicity. This is equivalent to assuming that for a given growth regime the relevant factor (a length) is independent of n, p, and T, which appears to be a fair approximation.[5]

Criterion for Extended Chain Growth. So far the approach is quite general and the expressions given above must be adapted to the particular system and conditions considered. Various applications of the theory have been proposed for the growth of PEO crystals by Buckley,[19] Labaig,[20] and Lauritzen,[22] differing essentially in the evaluation of the energy barriers for the formation of the growth nucleus. These treatments are based on detailed models of the chain conformation in the growth nuclei of different length and thus involve some arbitrariness in the estimation of the relevant basal surface free energies (σ_e and $\bar{\sigma}_e$). In order to avoid such ambiguities, we will first search for conditions under which the length of the bidimensional growth nucleus should be equal to L, thus giving rise to extended chain crystals.

In once folded chain crystals, with chain ends rejected onto the surface layers of the lamella, one has (Figure 2b)

$$\sum_e(n = 1) = 2\sigma_{e,e}(n = 1) + 2\sigma_{e,f} \quad (15)$$

where $\sigma_{e,e}(n = 1)$ is the surface free energy contribution of one chain end in a composite surface involving $n = 1$, and $2\sigma_{e,f}$ is the surface free energy of one chain fold, the value of which is assumed here to be independent of n.

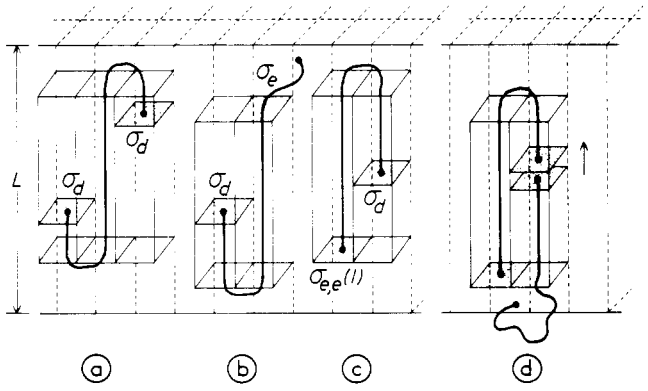

Figure 3. (a–c) Possible chain conformations in growth nuclei of length $L/2 < l < L$ and the relevant end-surface free energies. (d) Unfolding mechanism of once folded chains in contact with an extended chain substrate and with the melt (cf. Figure 7 in ref 8). The arrow indicates the direction of the force driving the pair of chain ends inside the crystal lattice.

Such crystals melt at $T_m(1,p)$, where according to eq 11 one has

$$abL\Delta h_f[T_m(\infty) - T_m(1,p)]/T_m(\infty) - kT_m(1,p) \ln p = ab\sum_e(n = 1) + kT_m(1,p) \ln C \quad (16)$$

This expression is identical with that established by Buckley and Kovacs[14] on purely thermodynamic considerations and defines the variation of the melting temperature of once folded chain crystals as a function of p (or L) for which $\sum_e(n = 1)$ is an invariant (see Appendix I).

Clearly, above $T_m(1,p)$ the growth nucleus must have a length $l > L/2$ and thus involve at most two folds per chain. Although a great many situations may be considered, as depicted schematically in Figure 3a–c, they all include either point defects inside the lattice (characterized by the surface free energy σ_d) or a cilium (σ_e) rejected outside the substrate which presumably both give rise to surface free energies larger than $\sigma_{e,e}(n = 1)$. With this assumption one should have in the temperature interval $T_m(1,p) < T < T_m(0,p)$, where $L/2 < l = L(1 + \bar{n})^{-1} < L$ (cf. eq 15)

$$\sum_e(0 < \bar{n} < 1) > 2\sigma_{e,f} + 2\sigma_{e,e}(n = 1) \quad (17)$$

Since in this temperature range the crystallization free energy of one chain is smaller than that at $T_m(1,p)$ (cf. eq 16), the inequality required for growth (eq 10) can only be satisfied for extended chain attachment for which $\sum_e(n = 0) = 2\sigma_{e,e}(n = 0) < 2\sigma_{e,e}(n = 1)$. In fact, for the PEO crystals considered[14] $\sigma_{e,e}(n = 0)$ is smaller than $\sigma_{e,e}(n = 1)$ (cf. Appendix I).

Assuming the surface free energy σ_d (cf. Figure 3) to be smaller than $\sigma_{e,e}(n = 1)$ would merely raise the lower limit of the relevant temperature interval somewhat above $T_m(1,p)$. There is, however, some suggestion that the lower limit (above which growth is induced by extended chain nuclei) should lie below $T_m(1,p)$ rather than above it.

Experimental evidence shows, in fact, that in once folded chain lamellae, the radial rate of advance $G_\phi(p)$ of full chain extension, around an extended chain seed, is greater than the rate $G(1,p)$ of deposition of once folded chains, whenever $T > T_\phi$.[8-10] Here T_ϕ is defined by the temperature at which $G_\phi(p) = G(1,p)$ and it is located between $T^*(0,p)$ and $T_m(1,p)$. Such chain extension consists of the migration of one chain end across the crystal while reeling in simultaneously another chain from the melt into the lattice vacancy left by the former[8] (cf. Figure 3d). This unfolding process thus incorporates all the situations intermediate between the original (once folded) and the final (extended) chain conformations. In the range $T > T_\phi$, therefore, crystal growth cannot proceed by deposition of folded chains, since full chain extension is more rapid and becomes the rate-controlling step, provided that the substrate is large enough to accomodate extended chains. Under this condition, extended chain crystals actually grow faster than once folded ones in the entire range within $T^*(0,p)$ and $T_m(0,p)$ (cf. Figure 1).

The argument developed above (cf. eq 17) can also be applied for the growth of n-times folded chain crystals within the interval $T_m(n + 1,p) < T < T_m(n,p)$, yielding

$$\sum_e(n + 1 > \bar{n} > n) > 2n\sigma_{e,f} + 2\sigma_{e,e}(n \geq 1) \quad (17a)$$

Nevertheless, for folded chain deposition the ratio $\sum_e(n + 1)/\sum_e(n)$ decreases and approaches unity as n increases (cf. Appendix I), thus resulting in a less determinantal free energy balance than that implied by extended chains. It should also be recalled that eq 17 and 17a have been derived by assuming the length of the successive stems remains invariant.[5]

Growth Rate of Extended Chain Crystals. According to the above conclusion, in the temperature interval $T_m(1,p) < T < T_m(0,p)$, the most probable length for the growth nucleus is equal to L (provided that the substrate is large enough). The lower limit of this temperature range may be, however, slightly lower or higher than $T_m(1,p)$ depending on whether σ_d is larger or smaller than $\sigma_{e,e}(1)$, respectively. Whatever the case, in the relevant range one can merely consider in the expression of the total flux (eq 13) of chain deposition the single term $S(L)$, corresponding to growth nuclei made of extended chains.

Under these conditions, the surface free energies σ_e and $\bar{\sigma}_e$ are both equal to $\sigma_{e,e}(n = 0) \equiv \sigma_{e,e}(0)$ and $\alpha = \alpha'$. Hence, the relevant attachment and detachment rates determining $S(L)$ can be expressed (cf. eq 5–8) by

$$A_0 = \beta \exp\{-[2bL\sigma - \psi\Delta F_c(L,T) + \alpha 2ab\sigma_{e,e}(0)]/kT\} \quad (18)$$

$$A = \beta \exp\{[\psi\Delta F_c(L,T) - \alpha 2ab\sigma_{e,e}(0)]/kT\} \quad (19)$$

$$B_1 = B = \beta \exp\{-[(1 - \psi)\Delta F_c(L,T) - (1 - \alpha)2ab\sigma_{e,e}(0)]/kT\} \quad (20)$$

Accordingly, for growth regime I, one has (eq 12 and 14)

$$G_I(0,p) \propto S(L) \propto A_0(A - B)/A = A_0[1 - (B/A)] \quad (21)$$

whereas for regime II

$$G_{II}(0,p) \propto [S(L)(A - B)]^{1/2} \propto (A_0 A)^{1/2}[1 - (B/A)] \quad (22)$$

Substituting for $\Delta F_c(L,T)$ its expression derived from eq 3 and 4 and using eq 21 and 22, one can write in a quite general manner

$$G_i(0,p) \propto \beta(p) \exp\left(-\frac{2ibL\sigma}{kT}\right) \exp\left[\frac{\psi abL\Delta h_f\Delta T}{kT_m(\infty)T} - \psi' \ln Cp - \frac{\alpha 2ab\sigma_{e,e}(0)}{kT}\right]\left\{1 - \exp\left[\frac{2ab\sigma_{e,e}(0)}{kT} - \frac{\Delta F_c(L,T)}{kT}\right]\right\} \quad (23)$$

in which $i = 1$ for mononucleated growth and $i = {}^1/_2$ for the multinucleated growth regime. For the sake of generality, the apportionating factor ψ is allowed here to take a value $\psi' \neq \psi$ for weighting the contribution of the localization entropy ($k \ln Cp$) to $\Delta F_c(L,T)$. In addition $\beta(p)$ is allowed to depend on the chain length, obeying a relationship similar to that displayed by the reciprocal shear

viscosity of low molecular weight PEO melts,[16] viz.,

$$\beta(p) = Jp^{-\gamma} \tag{24}$$

in which frequency factor J is assumed to be insensitive to small temperature changes and the exponent γ can take any value between zero and unity.[27] Note also that the last factor in eq 23, representing $[1 - (B/A)]$, is independent of i (cf. eq 21 and 22). The value of this factor is generally close to unity (cf. eq 10), except in the immediate vicinity of $T_m(0,p)$, where it rapidly vanishes (cf. eq 11).

An Unbiased Evaluation of the Lateral Surface Free Energy

The procedure usually adopted for testing the theoretical expression of G consists of considering the unknown parameters (σ, ψ, ψ', α, and γ in eq 24) as adjustable and substituting for them appropriate values to fit the experimental data. Since such a procedure involves a great deal of arbitrariness, it appears more expedient to express G in terms of an appropriate reduced variable enabling direct comparison of the data obtained with any pair of PEO fractions investigated. In fact, eq 23 provides an immediate route for such a comparison.

Consider the growth rates $G(0,p_1)$ and $G(0,p_2)$ of extended chain crystals for two fractions (labeled by 1 and 2) at two temperatures T_1 and T_2, both located in the range where extended chain nuclei are predominant, such that

$$p_1[T_m(\infty) - T_1]/T_1 = p_2[T_m(\infty) - T_2]/T_2 \equiv \theta \tag{25}$$

in which θ can take any value within the range $2.15 < \theta < 3.7$, where it can be uniquely associated with a measured value of $G(0,p)$ for each of the PEO fractions investigated (cf. Figure 1 and Table I).

Since $p = L/l_u$ (cf. eq 1), one can see that, for fixed values of θ, the exponential argument $\psi abL\Delta h_f\Delta T/kTT_m(\infty)$ in eq 23 is independent of the fraction considered, while $\alpha 2ab\sigma_{e,e}(0)/kT$ depends only slightly upon the particular values of T_1 and T_2, since in the relevant range of θ, $|T_1 - T_2|$ is smaller than 12 K. Furthermore, it can be shown easily that the value of the last factor in the expression of $G_i(0,p)$, representing $[1 - (B/A)]$, is nearly equal to unity, provided that neither T_1 nor T_2 is located in the immediate vicinity of $T_m(0,p)$, in other words (cf. eq 10) when $abl_u\Delta h_f\theta - kT \ln p$ is appreciably greater than $2ab\sigma_{e,e}(0) + kT \ln C$ ($\simeq 1.1 \times 10^{-13}$ erg; cf. Appendix I).

Under these conditions, eq 23 and 24 yield

$$\left.\frac{G_i(0,p_1)}{G_i(0,p_2)}\right|_\theta \simeq (p_1/p_2)^{-(\gamma+\psi')} \exp\left[-\frac{2ibl_u\sigma}{kT_m(\infty)}(p_1 - p_2)\right] \tag{26}$$

the right-hand side of which is independent of both T and θ. Accordingly, one can state the following *reduction rule*: the logarithmic growth rate branches $G(0,p)$ of extended chain crystals, obtained with low molecular weight PEO fractions (or similar materials), plotted against the reduced undercooling $\theta = (p/T)[T_m(\infty) - T]$, are superposable within a fair accuracy by means of vertical shifts, except in the vicinity of the relevant melting temperatures $T_m(0,p)$, where $G(0,p)$ vanishes.

One can also derive from the same argument a similar reduction rule for the growth rate branches $G(n,p)$ of n-times folded chain crystals by referring to fixed values of the relevant reduced variable: $\theta(1 + n)^{-1}$. In this case θ may take values corresponding to the range of overlap for the two fractions considered (cf. Figure 1), provided that for both growth is initiated by n-times folded chain nuclei. Hence at fixed θ, the expression for the ratio $G_i(n,p_1)/G_i(n,p_2)$ is similar to eq 26, but it involves an exponential argument reduced by the factor $(1 + n)$. As a consequence, for a given pair of fractions, the vertical separation of the successive logarithmic growth branches should decrease in a stepwise manner as n increases.

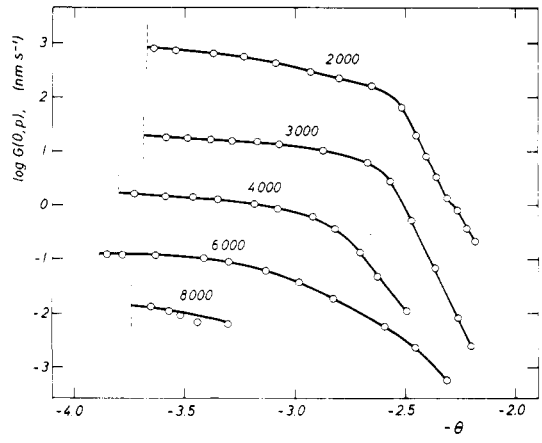

Figure 4. Dependence of the growth rate of extended chain crystals, $G(0,p)$, on the reduced undercooling, $\theta = p\Delta T/T$, and on chain length. Vertical dashed lines indicate values of θ corresponding to the relevant growth transition temperatures $T^*(0,p)$.

Nevertheless, as mentioned above, the theoretical argument resulting in a single type of growth nucleus of length $L(1 + n)^{-1}$ becomes less strict as n increases. In fact, the average surface free energy (per unit area) in folded chain crystals

$$\bar{\sigma}_e(n) = [\sigma_{e,e}(n) + n\sigma_{e,f}](1 + n)^{-1} \tag{27}$$

decreases and becomes insensitive to the number of folds when n is larger than 1 or 2 (cf. Appendix I). Hence growth can be initiated by nuclei of different length which all contribute to the total flux (cf. eq 13) determining $G_i(n,p)$. Relevant expressions of the latter have been given by several authors.[19,20,22]

Comparison with Experiment. The reduction rule for the growth branches $G(0,p)$ is well supported by the experimental data obtained with the fractions a–d, as shown in Figure 4 on an enlarged scale in the relevant range of θ. The vertical separation between any two $G(0,p)$ branches is defined by eq 26, from which one can easily determine $i\sigma$, viz.,

$$i\sigma = \frac{2.303kT_m(\infty)}{2bl_u(p_2 - p_1)}\left[\log \left.\frac{G(0,p_1)}{G(0,p_2)}\right|_\theta - (\gamma + \psi')\log\frac{p_2}{p_1}\right] \tag{26a}$$

since the values of the relevant parameters, other than γ and ψ', are known (cf. Table I and Appendix I).

Note that eq 26 is independent of θ, implying that the various $G(0,p)$ branches can be superimposed as a whole over the entire overlapping range of θ, with the exclusion of the neighborhood of the respective melting temperatures $T_m(0,p)$, where eq 26 becomes inapplicable. Figure 4 shows that this theoretical requirement is fairly well satisfied, suggesting that the growth nuclei actually consist of extended chains[28] whenever $T > T^*(0,p)$. Hence, the value of $i\sigma$, as derived from eq 26a, will be practically independent of the value of θ chosen for comparing the various growth branches shown in Figure 4.

For the unknown parameters two limiting situations might be envisaged by assuming either $\gamma = \psi' = 0$ or $\gamma = \psi' = 1$, which would result in the largest and in the smallest values of $i\sigma$, respectively. The corresponding ranges of $i\sigma$ are listed in Table II, as derived for $\theta = 3.0$, lying approximately in the middle of the common θ interval

Table II
Range of Variation of the Apparent Values of the Lateral Surface Free Energy $i\sigma$ (in ergs cm^{-2}) as Derived from the Growth Rate $G(0,p)$ of Extended Chain PEO Crystals at $\theta = 3.0^a$ (cf. eq 26a)

	POE		
	2000	3000	4000
3000	2.4 → 3.1		
4000	1.9 → 2.5	1.5 → 2.0	
6000	1.3 → 1.8	1.0 → 1.4	0.8 → 1.1

[a] $i = 1$ for growth regime I; $i = 1/2$ for growth regime II. Minimum and maximum values were obtained with $\gamma = \psi' = 1$ and $\gamma = \psi' = 0$, respectively.

for $n = 0$ (cf. Figure 4). These $i\sigma$ ranges each refer to the pair of fractions compared, as indicated in the relevant column and line. The intermediate and most realistic assumption $\gamma = 0$ and $\psi' = 1$ (or conversely) would yield approximately the average of the extreme values of $i\sigma$ given in Table II.

It can be noticed immediately that these values are much smaller than those usually reported[5] and moreover they increase by a factor of about 3 when the average chain length (at constant p_1/p_2) is reduced by 2. This suggests that the "apparent" value of $i\sigma$ is reciprocally related to the chain length. These findings are, of course, inconsistent with the theoretical model, implying σ to be independent of the chain length. Furthermore, such low values of σ appear to be physically meaningless for characterizing the sharp boundary between a crystalline substrate and the melt. Finally, the data given in Table II reveal that the discrepancy between theory and experiment is irreducible by any adjustment of the values of the unknown parameters γ and ψ.

It may be argued that these discrepancies originate from the various approximations introduced in deriving eq 26, in particular from the reduction of the total flux (eq 13) to a single term $S(L)$. It can be shown, however, that taking into account all the factors involved in eq 23 and allowing J (eq 24) to depend on temperature[16] would not modify the data given in Table II by more than about 5%, which is comparable to the scatter introduced by comparing the growth branches $G(0,p)$ at extreme values of θ rather than at $\theta = 3.0$. Furthermore, assuming for the growth nuclei an average length lying between $L/2$ and L[28] would merely increase the limiting values of $i\sigma$ listed in Table II by a factor less than 2, without suppressing their variation with the chain length. These results thus justify the use of the approximations made above and confirm again the irreducibility of the discrepancy between theory and experiment.

A similar procedure has also been applied for the growth branches of once folded chain crystals (fractions c–f, in Table I), for which the above reduction rule still appears to hold with fair accuracy (cf. Figure 1) within the common θ range. The relevant values of $i\sigma$ are then given by eq 26a by multiplying its right-hand side by the factor $1 + n = 2$. As anticipated above, one would expect the vertical separation of the $G(1,p)$ branches (at fixed θ) to be reduced by about the same factor in order to maintain the value of $i\sigma$ invariant. Figure 1 shows, however, that this theoretical requirement is not satisfied, since the vertical separation of the $G(1,p)$ growth branches is essentially the same as (actually slightly larger than) that of the $G(0,p)$ branches. This implies that, at constant γ and ψ', the apparent values of $i\sigma$ for $n = 1$ are about twice as large as those for $n = 0$. Furthermore, Figure 1 shows that the same situation prevails for the $G(2,p)$ growth branches, thus resulting for $n = 2$ in about three times larger $i\sigma$ values than for extended chain crystal growth.

These findings suggest that, at constant p, the apparent values of $i\sigma$ are approximately proportional to $1 + n$, while at constant n they decrease with increasing p (see above), in a way similar to the variation of the reciprocal lamellar thickness (eq 1). In other words, the overall lateral surface free energy, $2bl\sigma$, generated by the attachment of the first stem (cf. eq 2) does not appear to be proportional to the length of the latter but varies appreciably more slowly than l. This is, of course, in contradiction with the basic model of coherent surface nucleation (cf. Figure 2a), a conclusion which will be further substantiated in the next section.

Temperature Dependence of the Growth Rate at Fixed Chain Length. The thermal variation of $G(n,T)$, at fixed p, will now be analyzed with the use of the following assumptions: (i) the length l_n of the growth nuclei is always an integer submultiple of the chain length, i.e., $l_n = L(1 + n)^{-1}$, and its value increases stepwise with T at each growth transition temperature $T^*(n,p)$ in a way similar to the lamellar thickness, and (ii) $B = B_1$, thus $\alpha = \alpha'$ (cf. eq 6 and 8). Under these conditions, within each temperature interval where n is invariant, the total flux (eq 13) can be reduced to a single term $S(l_n)$, and $G_i(n,T)$ can be expressed similarly to eq 21 and 22, viz.,

$$G_i(n,T) \propto (A_0/A)^i A[1 - (B/A)] \tag{28}$$

in which $i = 1$ or $1/2$ for mono- or multinucleated growth regime, respectively. Substituting for A_0/A the relevant expressions given in eq 5 and 7 yields

$$G_i(n,T) \propto A[1 - (B/A)] \exp\{-[2bl_n\sigma + \alpha 2ab(\sigma_e - \bar{\sigma}_e)](i/kT)\} \tag{29}$$

in which the average surface free energy $\bar{\sigma}_e \equiv \bar{\sigma}_e(n)$ is defined by eq 27 and (cf. eq 7 and 8)

$$A \equiv A(n,T) = \beta \exp\{[\psi \Delta F_c(l_n,T) - \alpha 2ab\bar{\sigma}_e(n)]/kT\} \tag{30a}$$

$$B \equiv B(n,T) = \beta \exp\{-[(1 - \psi)\Delta F_c(l_n,T) - (1 - \alpha)2ab\bar{\sigma}_e(n)]/kT\} \tag{30b}$$

At fixed p (and L), it is convenient to compare the growth rates at various values of n and T selected in such a way that

$$A(n,T) = A(n',T'); \qquad |n - n'| = 1, 2, \ldots \tag{31}$$

thus involving the same fixed value of the (new) reduced variable (cf. eq 30a)

$$\phi(n,T) \equiv \{\psi \Delta F_c[L(1 + n)^{-1},T] - \alpha 2ab\bar{\sigma}_e(n)\}(kT)^{-1} \tag{32}$$

in each temperature interval where n is invariant. In fact, due to the discontinuities displayed by the variation of ϕ with n and T at each growth transition temperature $T^*(n,p)$, there is a range within each temperature interval (where n is constant) which corresponds to a common range of ϕ, provided that ψ and α are not both equal to zero (an unrealistic case).

By adopting for the relevant thermodynamic parameters defining $\phi(n,T)$ the values given by Buckley and Kovacs[13,14] (see Appendix I) and assuming, for simplicity, $\psi = \alpha > 0$, one can plot for each fraction the actual growth rate $G(n,T)$ as a function of the reduced variable ϕ/ψ (cf. eq 32, with $\psi = \alpha$). Figure 5 shows such a plot for the fraction d(6000) and defines the common range of ϕ/ψ within which one can compare, at fixed ϕ, a set of $G(n,T)$ values satisfying eq 31. Concomitantly, any fixed value of ϕ/ψ uniquely defines a set of temperatures T_n (each associated with the relevant value of n) at which eq 31 is satisfied. A series of such temperatures is listed in the first line of Table III,

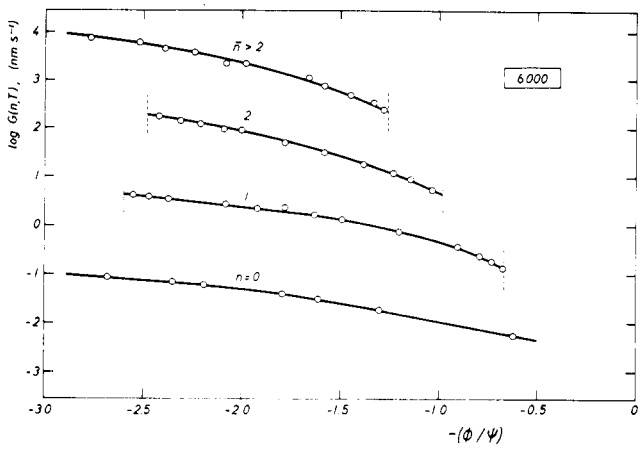

Figure 5. Dependence of the crystal growth rate $G(n,T)$ of the d(6000) fraction on the reduced variable $\phi(n,T)$, defined by eq 32 and determined by using the values of the relevant parameters listed in Appendix I (including their temperature dependence). Vertical dashed lines indicate ϕ/ψ values corresponding to the relevant growth transition temperatures $T^*(n)$.

Table III
Corresponding Temperatures and $i\sigma$ Values as Derived from the Temperature Dependence of the Growth Rate $G(n,T)$ of the d(6000) PEO Fraction for ϕ/ψ = 1.75 and Assuming $\alpha = \psi$ (cf. eq 32 and 33)

	n			
	0	1	2	3
T_n, °C	61.57	57.56	54.12	50.54
$i\sigma$, erg/cm²		1.05	2.58	5.36

as derived for $\phi/\psi = 1.75$, lying in the middle of the common ϕ/ψ interval for the fraction considered. Note also that the set of temperatures T_n, corresponding to *any* fixed value of ϕ/ψ in the range of overlap (Figure 5), are all located sufficiently far below the relevant melting temperatures $T_m(n,p)$, at which $\phi = 0$, so that in eq 29 the ratio $B/A \simeq 0$ and can be neglected.

Under these conditions, one can express the ratio of the growth rates observed at any two corresponding temperatures T_n, involving the same value of ϕ, by (cf. eq 29)

$$\left.\frac{G_i(n,T)}{G_i(n',T')}\right|_\phi \simeq \exp\left\{-\frac{2ibL\sigma}{k}\left[\frac{1}{(n+1)T}-\frac{1}{(n'+1)T'}\right]\right\} \quad (33)$$

in which the term $\alpha 2ab[\sigma_e - \bar{\sigma}_e(n)]$ has been neglected in the exponential argument. This appears to be a fair approximation since $L(1+n)^{-1} \gg a$, implying the first term in the exponential argument of eq 29 to be predominant (which is equivalent to assuming $\sigma_e \simeq \bar{\sigma}_e$).

Note also that the right-hand side of eq 33 is independent of ϕ and depends only slightly upon T. Therefore the various $G(n,T)$ growth branches plotted against ϕ/ψ should be superposable merely by vertical shifts over the entire overlapping ϕ range. Figure 5 shows that this theoretical requirement appears to be approximately fulfilled, since the various $G(n,T)$ branches are nearly parallel, though those relevant to $n \leq 1$ and $n \geq 2$ display some divergence. Thus at fixed p, eq 33 defines a reduction rule similar to that derived above for fixed n (cf. eq 26) and provides a convenient means for determining the apparent values of $i\sigma$ by comparing the actual growth rates at any set of temperatures T_n associated with a fixed value of ϕ in the common range. The $i\sigma$ values listed in the second line of Table III result from such a comparison (for $\phi/\psi = 1.75$) of the successive pair of $G(n,T_n)$ values, such

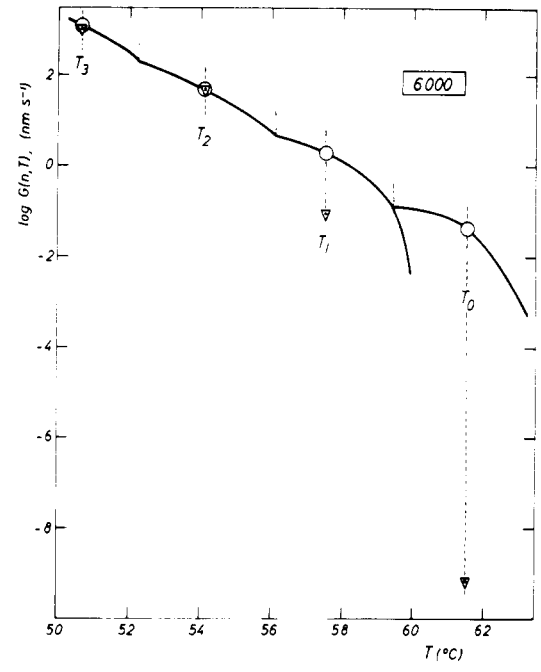

Figure 6. Temperature dependence of the crystal growth rate $G(n,T)$ of the d(6000) fraction (solid line). Vertical dashed lines indicate the set of corresponding temperatures T_n listed in Table III. Vertical dotted lines, growth transition temperatures $T^*(n)$; triangles, theoretical values of $G_i(n,T_n)$, as derived from eq 29, with $i\sigma = 5$ erg cm^{-2} and by using the procedure described in the text, with $Q = 7.29$.

that $|n'-n| = 1$. In considering other ϕ/ψ values, only the intermediate value of $i\sigma$ would undergo some significant modification, due to the slight divergence between the $G(1,T)$ and $G(2,T)$ growth branches (Figure 5).

Although the approximation made above ($\sigma_e - \bar{\sigma}_e \simeq 0$) results in a slight overestimation of $i\sigma$, since σ_e is presumably larger than $\bar{\sigma}_e(n)$, the data given in Table III essentially confirm the conclusion reached above, e.g., the apparent values of $i\sigma$ are too small at low values of n and they rapidly increase with decreasing lamellar thickness, attaining acceptable values at relatively large undercoolings. Similar analysis made with the other fractions leads to the same conclusion.

The discrepancy between theory and experiment is further illustrated in Figure 6 which depicts the temperature dependence of $G(n,T)$ displayed by the d(6000) fraction, with the indication (by vertical dashed lines) of the T_n values listed in Table III. In addition, the triangles show the quantity $-(2/2.3)ibL\sigma/(n+1)kT_n + Q$, determining the theoretical values of log $G(n,T_n)$, as derived from eq 29 (with $\sigma_e \simeq \bar{\sigma}_e$). The constant Q has been adjusted here to bring the calculated and experimental values of log $G(2,T_2)$ into coincidence whereas the value of $i\sigma$ has been assumed to remain independent of n and to amount to 5 ergs cm^{-2}, which is comparable to that derived above at relatively large undercoolings (see Table III).

Figure 6 shows that the ratio of the experimental and calculated values of $G(n,T_n)$ dramatically increases (by many orders of magnitude!) as n decreases. In fact, the experimental data at the successive corresponding temperatures (shown by circles) define a fairly straight line whereas the calculated $G_i(n,T_n)$ values lie on a hyperbolic curve displaying a strong downward curvature. This figure clearly illustrates the effect of the discrepancies reported above and shows that the latter cannot be removed by any adjustment of the values of $i\sigma$ or ψ or α. In fact, a lower value of $i\sigma$ would merely shift the parallel section of the theoretical and experimental curves of log $G(n,T_n)$ to

higher temperatures (cf. Table III) whereas assuming $0 < \psi \neq \alpha > 0$ would shift only slightly the values of the corresponding temperatures T_n obtained with $\psi = \alpha$ (Table III). Hence, none of these modifications would affect the overall hyperbolic outline of the theoretical curve, in contrast with the straight line envelope displayed by the experimental log $G(n,T)$ data in the relevant undercooling range (cf. Figure 6).

It can also be shown that this fundamental discrepancy cannot be removed by taking into account growth nuclei other than those involving integer values of n, as assumed above. In the temperature interval where n-times folded chain crystals grow, this procedure would merely reduce the average length of the growth nuclei to $l_{\bar{n}} < l_n$, where $l_{\bar{n}}$ is defined by $L/(1 + \bar{n})$, with $\bar{n} > n$. For a given fraction, one can thus compare the growth rates at various temperatures $T_{\bar{n}}$, corresponding again to a fixed value of the reduced variable (eq 32) such that, on the average, $A(\bar{n},T) = A(\bar{n}',T')$ (eq 31). In these conditions, and imposing for simplicity $|\bar{n}' - \bar{n}| = 1$, eq 33 can be written as

$$\log \left.\frac{G_i(\bar{n}+1,T')}{G_i(\bar{n},T)}\right|_{\phi} \simeq \frac{2ibL\sigma}{2.303k}\left[\frac{1}{(\bar{n}+1)T} - \frac{1}{(\bar{n}+2)T'}\right] \tag{33a}$$

the left-hand side of which is practically independent of $\bar{n}$ whereas the second factor in the right-hand side rapidly increases as $\bar{n}$ decreases, thus implying a decrease of $i\sigma$ with increasing lamellar thickness. Conversely, for fixed values of $i\sigma$, the overall thermal variation of log $G(\bar{n},T)$ becomes hyperbolic rather than being linear (cf. Figure 6). The various approaches based on detailed model calculations[19,20,22] all display this general trend and, for reasonable values of $i\sigma$, they extend the thermal variation of $G(\bar{n},T)$ to a much wider range than that actually observed.

Discussion

The $i\sigma$ values listed in Tables II and III have been derived from the straightforward application of the classical theory (adapted for short chains) to a coherent set of experimental data for which most of the relevant parameters (including the lamellar thickness) are known, while allowing the others to take extreme values. As already mentioned above, these values of σ are much smaller than those derived from primary nucleation in molten PEO droplets[23] ($\sigma \geq 30$ erg cm^{-2}) or from an empirical relationship given by Lauritzen and Hoffman:[17] $\sigma = 0.1\Delta h_f(ab)^{1/2}$ ($\simeq 11.1$ erg cm^{-2}, for PEO crystals). There is, of course, no necessity for σ to take the same value at the surface of a tiny molecular bundle as for a single stem deposited on a smooth surface, though again fair agreement has been claimed for polyethylene.[5,21]

Furthermore, the value of $i\sigma$ appears to vary as the inverse of the lamellar thickness (cf. eq 1), since at constant p it increases as $n + 1$ and at constant n it decreases with increasing p, instead of remaining invariant as required by the theoretical model (cf. Figure 2a and eq 2).

It should be pointed out that the lateral surface free energy is an essential parameter in all kinetic theories based on coherent surface nucleation,[1-3] since chain folding (i.e., lamellar thicknesses $l < L$) can only be expected when $\Delta\phi_0$ is positive (eq 2). In fact, the theory predicts a dramatic increase for both l and G (often referred to as the δl catastrophe[17]) when $\Delta\phi_0$ becomes negative, i.e., when

$$\psi\Delta F_c > 2bl\sigma + \alpha 2ab\sigma_e \tag{34}$$

which may always arise when the crystallization temperature is low enough. The critical undercooling ΔT_c at which $\Delta\phi_0 = 0$ can thus be defined by (cf. eq 3 and 4)

$$\Delta T_c = \frac{T_m(\infty)}{\Delta h_f}\left[\psi^{-1}\left(\frac{2\sigma}{a} + \alpha\frac{2\sigma_e}{l}\right) + \frac{kT_c}{abL}\ln Cp\right] \tag{35}$$

where the contribution of the ln Cp term rapidly decreases as $L = pl_u$ increases, and even for the present systems its contribution to ΔT_c is small as compared with those resulting from the surface free energy terms. Although in the absence of reliable values of the latter the value of ΔT_c cannot be evaluated accurately, experimental evidence shows a leveling off at low temperatures ($T < 300$ K) for both l and G, rather than an increase[9] (cf. Figure 1).

The nature of the failure of the theoretical predictions suggests that the major discrepancies originate from the incorrect evaluation of the free energy barrier $\Delta\phi_0$ (eq 2) opposing the crystallographic attachment of the first stem. Nevertheless, the failure of the second postulate of the theory, i.e., the sequential deposition of the consecutive stems of fixed length, resulting in eq 12, cannot be ruled out. In fact, the above analysis is explicitly based on this postulate (cf. eq 21, 22, and 28), the validity of which cannot be ascertained unambiguously in considering the present growth rate data. One must thus conclude that *at least one* of the basic postulates of current theories,[1,17] as expressed by eq 2 and 12, is incompatible with the actual growth kinetics of low molecular weight PEO crystals in the bulk.

It should be pointed out, however, that the classical theory correctly predicts a few important features of the present PEO data, at least in a qualitative manner. For example, the theory predicts for integer values of n the existence of discrete growth branches and the relevant melting temperatures $T_m(n,p)$. In fact, the set of thermodynamic parameters (other than σ and σ_e) used in the above analysis has been determined from $T_m(n,p)$ data[14] (cf. Appendix I). The intersection of these growth branches further defines a set of discrete transition temperatures $T^*(n,p)$, at which the reduced variable ϕ (eq 32) abruptly increases as n takes the value of $n + 1$. The theoretical values of $T^*(n,p)$ are, however, significantly closer to $T_m(n,p)$ than the experimental ones, and more so as n decreases.[19] Furthermore, the various $G(p,\theta)$ and $G(n,\phi)$ growth branches as observed at fixed n and p, respectively, are superimposable within a fair accuracy (Figures 1, 4, and 5); nevertheless, their vertical separation, determined by the product $l\sigma$, does not obey the theoretical relationships (eq 26 and 33) involving a constant value of σ of reasonable magnitude. However, the latter becomes of the usual order of magnitude at large undercooling, at which the growth nuclei involve noninteger values of n and result in highly unstable[9] and relatively thin ($\simeq 10$ nm) lamellae, whatever the chain length.[14]

It should also be mentioned that the theory developed here for short chains readily applies to long chains, for which the entropy of localization (k ln Cp) vanishes as $L \to \infty$ and the effect of chain ends becomes negligible when n is large enough (cf. eq 27). The minimum fold length required for growth (eq 9) is then simply defined by $l_{min} = 2\sigma_{e,f}/\Delta f$ and leads to an analytical expression of the total flux S_T by assuming in eq 13 the upper limit of the integral to be ∞. These modifications yield the well-known and widely-used expression for the growth rate[5,24]

$$\ln G_i(T) = C_i(T) - 4ib\sigma\sigma_{e,f}T_m(\infty)/kT\Delta h_f\Delta T \tag{36}$$

where $C_i(T)$ incorporates all the terms which vary only slightly with T [in the range near $T_m(\infty)$], and its temperature dependence can be ignored. The second and most critical term in the right-hand side of eq 36 merely originates from the lateral surface free energy $2bl\sigma$ of the first

depositing stem (eq 2), with $l = l_{min} = 2\sigma_{e,f}T_m(\infty)/\Delta h_f \Delta T$ (cf eq 4). Thus the term dominating the thermal variation of $G_i(T)$ close to the melting temperature is precisely the one from which the various discrepancies listed above originate. The paradox clearly results from the strong temperature dependence of l_{min} ($\propto \Delta T^{-1}$) for long chains, which is equivalent to the effect resulting from successive growth transitions as T approaches $T_m(\infty)$. Application of eq 36 to the growth rate data obtained with a high molecular weight (~150 000) PEO sample[9] leads to the value of $i\sigma\sigma_{e,f} \simeq 225$ erg^2 cm^{-4}. Adopting for $2\sigma_{e,f} \sim 45$ erg cm^{-2} (cf. Appendix I) yields $i\sigma \simeq 10$ erg cm^{-2}, which is about twice as large as the greatest $i\sigma$ value derived from eq 33 for the fraction d(6000) (cf. Table III).

For short PEO chains the length of the growth nucleus ($l \leq L$) appears to be invariant within each temperature interval where n is an integer. One cannot expect, therefore, the individual growth branches to be described by a relationship similar to eq 36, based on a continuous variation of l_{min} proportional to ΔT^{-1}. The relevant expression is given by eq 29, which, together with eq 30a, can be reduced to

$$\ln G_i(n,T) = C_i'(n,T) + \psi abL\Delta h_f \Delta T/(n+1)kTT_m(\infty) \quad (37)$$

provided that in each temperature interval where n = constant, T ranges sufficiently far below $T_m(n,p)$, where the contribution of the ratio B/A to $\ln G_i$ is negligible. In eq 37, $C_i'(n,T)$ includes again all the terms which are relatively insensitive to temperature changes. These are separated from the last term which dominates the thermal variation of $G_i(n,T)$ and which is independent of the growth regime (i). Note that this term originates from the crystallization free energy $\Delta F_c(l,T)$ controlling the energy balance $\Delta\phi_0$ for the deposition of the first stem in eq 2. In fact, unlike the former case (eq 36), l is supposed here to take discrete values equal to $L(n+1)^{-1}$, rather than to vary as ΔT^{-1}. Accordingly, in each temperature interval and in a range not too close to $T_m(n,p)$, one would expect the negative slopes

$$-\mathrm{d}\ln G_i/\mathrm{d}T \simeq \psi abL\Delta h_f/(n+1)kTT_m(\infty) \quad (37a)$$

to be nearly proportional to $(n+1)^{-1}$. This is in fact observed for the *theoretically* derived growth branches, even when $\bar{n}$ is allowed to take fractional values[19,20] between n and $n+1$, while l_{min} ($=2\bar{\sigma}_e/\Delta f$) varies as ΔT^{-1}, similar to the case of long chains.

Equation 37a is, however, inconsistent with experiment, since for $n \geq 1$ the relevant slopes are practically independent of n, while for $n = 0$ they almost vanish above $T^*(0,p)$ rather than increase (cf. Figures 1 and 6). Clearly, this additional discrepancy originates from the postulate that the rate-controlling step of crystal growth consists of the deposition of the first, single stem of length l (cf. Figure 2a and eq 2) which is generally much smaller than L [in the present analysis this length has been approximated by $l_n = L(n+1)^{-1}$; cf. eq 29]. Thus according to eq 37, the subsequent deposition of the residual part of the chain ($L - l_n$) does not contribute appreciably to the thermal variation of $G_i(n,T)$, except when T closely approaches $T_m(n,p)$. This implication of the theoretical model is contradicted by experiment, as will be shown now.

In fact, at fixed p, the overall envelope of the actual $G(n,T)$ or $G(n,\theta)$ growth branches appears to be approximately a straight line (Figures 1 and 6). Interestingly, the slope $\mathrm{d}\ln G/\mathrm{d}\theta$ of these envelopes is of the same order of magnitude as the dimensionless ratio $\Delta S_f/k$, in which $\Delta S_f = abl_u\Delta h_f/T_m(\infty) \equiv \Delta H_f/T_m(\infty)$ represents the crystallization entropy of one monomer unit, ΔH_f being the relevant enthalpy (cf. Appendix I). Consequently, these envelopes satisfy the empirical relationship

$$\ln G(p,T) - C''(p,T) = \psi(p)(\Delta S_f/k)\theta = \psi(p)abL\Delta h_f\Delta T/kTT_m(\infty) \quad (38)$$

which is similar to eq 37 but does not involve any strong dependence on n. In fact, $\psi(p)$ ranges from 0.6 to 1, as p decreases from 227 to 63 (cf. Table I), while the new temperature-insensitive term $C''(p,T)$ includes an activation barrier which varies approximately as $p^{1/2}$, as derived from the vertical separation of the growth branches shown in Figure 1. (Note that the theoretically predicted separation should vary as $p(n+1)^{-1}$, cf. eq 26 and the relevant discussion.)

This empirical expression (eq 38) suggests that the rate-controlling step of crystal growth consists of the deposition of one molecule as a whole, rather than merely a segment of limited length (Figure 2a). Such a molecular nucleation model is under current investigation; its description is, however, beyond the scope of this paper.

Conclusion

Application of current kinetic theories to the crystal growth of low molecular weight PEO fractions reveals a series of fundamental discrepancies contradicting the model of coherent surface nucleation resulting in a sequential deposition of chain segments of fixed length. These findings, together with some recent data on chain conformation in polymer crystals revealed by neutron scattering, suggest that crystal growth may not involve a unique process but may depend critically on the crystallization conditions including, in addition to temperature and pressure, the environment of the depositing chains and their mobility during subsequent conformational rearrangements. The relevant molecular processes are certainly complex and result in most cases in compromises between various possibilities, leading eventually to unstable semicrystalline structures. In contrast, the systems analyzed in this paper display a remarkably simple model behavior which to some extent appears consistent with the theoretical model. Closer inspection and quantitative comparison of the theory with experiment reveal, however, that the actual data are incompatible with the basic postulates of currently accepted theoretical models, which thus need major revision.

Appendix I. Characteristic Parameters of PEO Crystals

Lattice Parameters.[12] The length of one monomer unit along the helical chain axis is $l_u = 0.2783$ nm. The cross-sectional area of the PEO chain is $s_0 = ab = 0.214$ nm^2. In the various calculations given in the text, it has been assumed, for simplicity, that $a = b = s_0^{1/2} = 0.463$ nm.

Thermodynamic Parameters.[13,14] The melting temperature of a large and perfect crystal, including neither chain folds nor chain ends, is $T_m(\infty) = 342.1$ K $\simeq$ (68.9 ± 0.4) °C. The enthalpy of fusion ΔH_f of one monomer unit at $T_m(\infty)$ amounts to 2.07 kcal/mol, thus $\Delta h_f = \Delta H_f/s_0 l_u N_A = 57.7$ cal cm^{-3} $\simeq$ 240 J cm^{-3}, while the corresponding entropy $\Delta S_f = \Delta H_f/T_m(\infty) = 6.05$ cal K^{-1}/mol and $\Delta S_f/R = 3.06$ eu; N_A is Avogadro's number and R is the gas constant.

Both ΔH_f and ΔS_f decrease with T, the excess heat capacity controlling the temperature dependence of ΔH_f being $\Delta C_p = 2.07$ cal K^{-1}/mol.

Surface Free Energies. The surface free energies of mature PEO crystals have been derived by Buckley and Kovacs[13,14] from the variation of the melting temperatures

$T_m(n,p)$ with n and p, while defining the free energy balance in molar quantities (cf. eq 3, 4, 10, and 11) as

$$\Delta F_c(l,T) - \sum_e(n) = 0 \quad \text{(A1)}$$

where

$$\sum_e(n) = 2\sigma_{e,e}(n) + 2n\sigma_{e,f} \quad \text{(A2)}$$

$\sigma_{e,e}(n)$ is the surface free energy of one chain end in the surface of a crystal made of n-times folded chains, and $2\sigma_{e,f}$ is the surface free energy of one chain fold (occupying two lattice sites, cf. Figure 2b). Hence

$$[p\Delta H_f/T_m(\infty)][T_m(\infty) - T_m(n,p)] - RT_m(n,p) \ln p = \sum_e(n) + RT_m(n,p) \ln C \equiv \sum_e^+(n) \quad \text{(A3)}$$

in which C^{-1} is the number of monomer units in the statistical segment.[15]

The analysis, at an average temperature $\bar{T} = 61.2$ °C, in the melting range of the various fractions considered, yields the following results

$$2\sigma_{e,e}(0) + R\bar{T} \ln C = 1.57 \text{ kcal/mol}$$

$$2\sigma_{e,e}(n \geq 1) + R\bar{T} \ln C = 2.15 \text{ kcal/mol}$$

$$2\sigma_{e,f} = 1.38 \text{ kcal/mol}$$

from which one can easily derive the various molar surface free energies $\sum_e^+(n)$. In most cases it was necessary to account for the temperature dependence of $\sum_e^+(n,T) = \sum_e^+(n,\bar{T})[1 - \alpha(T - \bar{T})]$ with $\alpha \simeq 1.3 \times 10^{-2}$ K^{-1}. (The conversion factor is 1 kcal/mol = 32.5 erg cm^{-2}.)

References and Notes

(1) J. I. Lauritzen, Jr., and J. D. Hoffman, *J. Chem. Phys.*, **31**, 1680 (1959); *J. Res. Natl. Bur. Stand., Sect. A*, **64**, 73 (1960).
(2) J. D. Hoffman and J. I. Lauritzen, Jr., *J. Res. Natl. Bur. Stand., Sect. A*, **65**, 297 (1961).
(3) F. C. Frank and M. Tosi, *Proc. R. Soc. London, Ser. A*, **263**, 323 (1961).
(4) A. Keller, *Philos. Mag.*, **2**, 1171 (1957).
(5) J. D. Hoffman, G. T. Davis, and J. I. Lauritzen, Jr., in "Treatise on Solid State Chemistry", Vol. 3, N. B. Hannay, Ed., Plenum Press, New York, 1976, Chapter 7, pp 497–614.
(6) D. M. Sadler and A. Keller, *Macromolecules*, **10**, 1128 (1977).
(7) A. J. Kovacs and A. Gonthier, *Kolloid Z. Z. Polym.*, **250**, 530 (1972).
(8) A. J. Kovacs, A. Gonthier, and C. Straupe, *J. Polym. Sci., Part C*, **50**, 283 (1975).
(9) A. J. Kovacs, C. Straupe, and A. Gonthier, *J. Polym. Sci., Part C*, **59**, 31 (1977).
(10) A. J. Kovacs and C. Straupe, *Faraday Discuss. Chem. Soc.*, in press.
(11) J. P. Arlie, P. Spegt, and A. Skoulios, *Makromol. Chem.*, **99**, 160 (1966); **104**, 212 (1967).
(12) Y. Takahashi and H. Tadokoro, *Macromolecules*, **6**, 672 (1973).
(13) C. P. Buckley and A. J. Kovacs, *Prog. Colloid Polym. Sci.*, **58**, 44 (1975).
(14) C. P. Buckley and A. J. Kovacs, *Colloid Polym. Sci.*, **254**, 695 (1976).
(15) P. J. Flory and A. Vrij, *J. Am. Chem. Soc.*, **85**, 3548 (1963).
(16) F. Pierson, Thesis, Faculté des Sciences, Université de Strasbourg, 1968.
(17) J. I. Lauritzen, Jr., and J. D. Hoffman, *J. Appl. Phys.*, **44**, 4340 (1973).
(18) I. C. Sanchez and E. A. Dimarzio, *J. Chem. Phys.*, **55**, 893 (1971).
(19) C. P. Buckley, *Polymer*, in press.
(20) J. J. Labaig, Thesis, University Louis Pasteur Strasbourg, 1978.
(21) J. D. Hoffman, G. S. Ross, L. Frolen, and J. I. Lauritzen, Jr., *J. Res., Natl. Bur. Stand., Sect. A*, **79**, 671 (1975).
(22) J. I. Lauritzen, Jr., private communication, 1975.
(23) J. A. Koutsky, A. G. Walton, and E. Baer, *J. Appl. Phys.*, **38**, 1832 (1967).
(24) R. L. Miller in "Flow-Induced Crystallization", R. L. Miller, Ed., Gordon and Breach, London, 1979.
(25) Shear viscosity measurements of molten PEO fractions[16] show that chain entanglements occur for molecular weights larger than about 7000.
(26) The apportionating of this entropy is not compulsory, since it can also be assumed to be entirely lost during the attachment of the first stem.[19] In the present context both assumptions lead to similar results.
(27) Experimental data do not suggest any molecular weight dependence for β, since the maximum of the growth rate (reached at room temperature) is independent of p[7,8] (cf. Figure 1).
(28) Or, they should involve a *fixed* fractional length ($^1/_2 < l/L < 1$) over the entire temperature range of interest, which appears to be an unrealistic assumption, since l/L must approach unity as T approaches $T_m(0,p)$.

The Effect of Preaveraging the Oseen Tensor on the Characteristic Frequency in Good Solvents

M. Benmouna and A. Ziya Akcasu*

Department of Nuclear Engineering, The University of Michigan, Ann Arbor, Michigan 48109.

Received December 6, 1979

ABSTRACT: The characteristic frequency $\Omega(q)$ for linear polymer chains is calculated as a function of temperature, for all values of q, without *preaveraging* the Oseen tensor. It is found that the preaveraging does not affect the overall qualitative behavior of $\Omega(q)$ as a function of q, but it introduces non-negligible numerical errors. In particular, in the intermediate q region and for good solvents the ratio $z(q) \equiv \Omega(q)/(k_BT/\eta_0)q^3$ is found to be 0.0789 instead of 0.071 which was previously calculated by using the preaveraged Oseen tensor. The ratio $z(q)$ is investigated in detail as a function of q.

The purpose of this paper is to investigate the effects of preaveraging the Oseen tensor on the characteristic frequency (or first cumulant) $\Omega(q)$ of the coherent scattering function $S(q,t)$ in a good solvent and to study the variation of $\Omega(q)/q^3$ with molecular weight and the type of polymer. $\Omega(q)$ was first calculated by Akcasu and Gurol[1] for a linear single unperturbed Gaussian chain without preaveraging the Oseen tensor. By comparing their results with those obtained by preaveraging the Oseen tensor, they concluded that the effect of preaveraging is to predict a lower value for $\Omega(q)$, with the difference being largest in the vicinity of $qa = 1$ and vanishing as $qa \to 0$. Akcasu and Higgins[2] later obtained $\Omega(q)$ for a freely jointed chain with nonpreaveraged Oseen tensor again in a Θ solvent. Burchard et al.[3] extended these calculations to branched polymers in a Θ solvent and showed that the error resulting from preaveraging may be as large as 40% in such polymers. More recently, Akcasu and Benmouna[4] considered

0024-9297/80/2213-0409$01.00/0